Title: Virtual Structural Health Monitoring and Remaining Life Prediction of Steel Bridges

Hajializadeh, D.[1], OBrien, E.J.[2,3] and O'Connor, A.J.[2,4]

[1]Anglia Ruskin University, UK , email: donya.hajializadeh@anglia.ac.uk

[2]Roughan O'Donovan Consulting Engineers, Ireland

[3]University College Dublin, Ireland, email: eugene.obrien@ucd.ie

[4]Trinity College Dublin, Ireland, email: OCONNOAJ@tcd.ie

Abstract

In this study a Structural Health Monitoring (SHM) system is combined with Bridge Weigh-in-Motion (B-WIM) measurements of the actual traffic loading on a bridge to carry out a fatigue damage calculation. The SHM system uses the 'Virtual Monitoring' concept, where all parts of the bridge that are not monitored directly using sensors, are 'virtually' monitored using the load information and a calibrated Finite Element (FE) model of the bridge. Besides providing the actual traffic loading on the bridge, the measurements are used to calibrate the SHM system and to update the FE model of the bridge. The newly developed Virtual Monitoring concept then uses the calibrated FE model of the bridge to calculate stress ranges and hence to monitor fatigue at locations on the bridge not directly monitored. The combination of a validated numerical model of the bridge with the actual site-specific traffic loading allows a more accurate prediction of the cumulative fatigue damage at the time of measurement and facilitates studies on the implications of traffic growth. In order to test the accuracy of the Virtual Monitoring system, a steel bridge with a cable-stayed span in the Netherlands was used for testing.

Key words: Virtual monitoring, Bridge FEM, Steel Bridges, Fatigue, SHM

Introduction

According to (Canadian Infrastructure 2016), $50 billion needs to be invested in the replacement and maintenance of bridges in 2016, spending $2 billion for bridges in poor/very poor condition, $11 billion for bridges in fair condition and $37 billion for bridges in good condition. Similarly, in the USA, $70.9 billion is needed to address the maintenance of more than 68 000 existing bridges. A difficult decision in the allocation of a maintenance budget lies in choosing the optimum intervals between inspections of bridge members (Lovejoy 2003). Structural Health Monitoring systems (SHMs) have great potential for optimising inspection intervals by monitor the loading and resistance of bridges in combination with structural modelling calibrated by measurements and can offer more accurate bridge safety assessments in a timely manner. An SHM system can secure structural and operational safety throughout the bridge life-cycle and issue early warnings of any deterioration or damage of a bridge prior to the need for costly repair or even catastrophic collapse. With 56% of bridges assessed every three years in Canada (Canadian Infrastructure 2016), utilising accurate SHM systems could result in significant savings.

Implementing accurate long-term SHM systems for bridges has been increasingly recognized in Canada (Desjardins et al. 2006; Mufti 2002; Cheung et al. 1997; Clarke 2014; Ghodoosipoor 2013), the USA (Saberi et al. 2016), Europe (Farreras-Alcover et al. 2016; Chellini et al. 2014; Dudás et al. 2015; Alampalli 2012; Cross et al. 2013), Japan (Sakagami 2015; Watanabe et al. 2014), China (Yan et al. 2016; Guo Tong et al. 2008), and elsewhere. Inaudi (2010) has conducted an overview of 40 bridge monitoring projects carried out in the period, 1996-2010, in 13 different countries including Austria, Belgium, Canada, Croatia, France, Germany, Italy,

Japan, Luxembourg, Russia, Sweden, Switzerland, Taiwan and the USA. This study suggests that all new bridge SHM projects are more or less evenly distributed between continents with a preponderance of European projects in the very first years of activity. Three main setbacks of SHM, however, are that: 1) monitoring data are only representative of a limited number of locations on structure monitored by sensors, 2) the financial constraints of covering all structural elements with the SHM system and 3) the cost associated with the duration of monitoring (Messervey et al. 2011).

The current study proposes the novel approach of 'virtual' monitoring for an orthotropic cable-stayed bridge in the Netherlands, in which a combination of direct measurement and numerical models is used to monitor some bridge elements directly and the rest virtually. This concept essentially can provide an SHM system that does not compromise on the number of locations monitored.

Among different types of bridge, the orthotropic steel deck (OSD), has been utilized successfully for thousands of bridges worldwide due to its notable advantages, namely, increased rigidity, material savings, suitability for standardization and prefabrication, etc (Guo et al. 2015). This type of bridge is widely used in Canada, the United States, the United Kingdom and other countries (Hammad et al. 2007; Yan et al. 2016; Inaudi 2010; Ye et al. 2014). In China alone, over 30 cable-stayed bridges with orthotropic deck systems were opened to the public from 2000 to 2014 (Wang et al. 2010; Ge & Xiang 2011).

A typical orthotropic steel bridge deck consists of a great number of welded joints (e.g., rib-to deck welded joints) vulnerable to fatigue-induced damage. Given that fatigue damage accumulation in decks and main superstructure elements is a common concern to bridge owners and management agencies, there is a high demand for effective fatigue life prediction

of fatigue-prone elements of orthotropic steel bridges to ensure bridge health and timely decision making for maintenance and rehabilitation planning. In recent decades, design specifications (AASHTO 2010, Eurocode 3 2005 , Canadian code (Canadian Institute of Steel Construction 2007)) and approaches to the prediction of remaining fatigue life of OSD bridges have been developed and applied actively in the context of reliable SHM systems (Battista et al. 2008; Guo & Chen 2011; Guo & Chen 2013; Guo et al. 2012; Guo et al. 2015; Kim et al. 2001; Anon n.d.; Liu et al. 2010; Ni et al. 2010; Okasha et al. 2012; Saberi et al. 2016; Orcesi & Frangopol 2013; Lu et al. 2016; Cross et al. 2013). Kolstein et al. (2007), in particular, present a review of typical fatigue details in orthotropic steel bridge decks and their corresponding testing programmes in European and Asian countries.

Recent literature has shown that SHM systems enable the measurement and recording of authentic long-term responses, providing a valuable tool for fatigue assessment and performance prediction (Frangopol et al. 2008; Guo Tong et al. 2008; Kwon & Frangopol 2010; Liu et al. 2010; Leander et al. 2010; Frangopol 2011). This concept has been investigated for different bridges and has resulted in different techniques for fatigue assessment. To name a few, Ni et al. (2010) proposed a fatigue reliability model which integrates the probability distribution of hot spot stress range with a continuous probabilistic formulation of Miner's damage accumulation using long-term monitoring data. The proposed technique has been tested on the Tsing Ma Bridge in Hong Kong. Liu et al. (2010) studied fatigue reliability assessment of retrofitting distortion-induced cracking in steel bridges, integrating monitored data based on the approach used in the AASHTO standard design specifications with all necessary information from finite element modelling (FEM). Guo & Chen (2011) have studied the field stress and measurement of two retrofitted details of a 50-year-old steel bridge

subjected to fatigue cracking to evaluate the effectiveness of the retrofits. Besides, probabilistic fatigue analyses are conducted to evaluate the reliabilities of these retrofitted details during their remaining service life. Guo et al. (2012) presented a fatigue reliability assessment of existing steel bridges subjected to fatigue cracking. The proposed approach is applied on a 50-year old bridge by using field monitored stress data collected by Mahmoud et al. (2006). Okasha et al. (2012) propose to use automated finite element model updating techniques as a tool for updating the resistance parameters of the structure, using monitored strain data obtained from crawl tests. Newhook & Edalatmanesh (2013) demonstrate the concepts of reliability and structural health monitoring (SHM) integrated in bridge assessment and decision systems. The bridge assessment model focusses on fatigue cracking issues associated with wheel loads due to heavy truck traffic. The fatigue reliability assessment method proposed by Guo et al. (2015) is based on a comprehensive vehicle load model and probabilistic multi-scale finite element (FE) analysis. Lu et al. (2016) then present a framework including deterministic finite-element-based hot-spot analysis and probabilistic modelling approaches to address the uncertainty-induced computational complexity. In addition, a learning machine integrating uniform design and support vector regression is used to substitute for the time-consuming finite-element model. Lee & Cho (2016) have applied a similar concept to perform probabilistic fatigue life prediction for bridges.

Reviewing recent studies conducted in the fatigue assessment field, there are mainly two approaches that are commonly used for fatigue damage evaluation and life prediction of steel bridge structures (Ye et al. 2014). The first is the traditional S-N curve method, in which the relationship between the constant-amplitude stress range, S, and the number of cycles to failure, N, is determined by appropriate fatigue experiments and described in an S-N curve.

It should be noted that the S-N method ignores local plastic effects and all strains are considered to be elastic. Also this method does not take account of pre-existing stress due to unusual geometry (Massarelli & Baber 2001). Despite the limitations of the classical *S-N* approach, it is considered as the basis for the current American Association of State Highway and Transportation official (AASHTO (2010)) design specifications, Eurocode 3 (2005) and the Canadian code (Canadian Institute of Steel Construction 2007). For constant amplitude stress cycles in the time history response, the fatigue design can be accomplished by referring to a typical *S-N* diagram. However, because real signals rarely conform to this ideal constant amplitude situation, an empirical approach is used for calculating the damage caused by stress signals of variable amplitude. When the response time history is irregular over time, a cycle counting method is used to decompose the irregular time history into an equivalent stress block of loading. The number of cycles in each block is recorded in a stress range histogram. The generated histogram is then used in association with the Palmgren-Miner rule (Miner 1945) to calculate the fatigue life.

The second approach to fatigue damage evaluation is fracture mechanics which explores issues of crack initiation and growth in the presence of a given stress field at the crack tip. In general, the two approaches are applied sequentially, with the S-N curve method being used at the bridge design stage or for preliminary evaluation of fatigue life and the fracture mechanics approach for more refined crack-based remaining fatigue life assessment or effective decision-making on inspection and maintenance strategies (Chryssanthopoulos & Righiniotis 2006). Generally, for the cases with no existing *S-N* curves, the Linear Elastic Fracture Mechanics (LEFM) approach has the potential to provide more flexibility. Besides, *S-N* curve-based approaches cannot incorporate the crack-size information, even if it were

known at the time of evaluation. Guo & Chen (2013) implemented long-term stress monitoring on several fatigue-prone details of a 40-year-old steel bridge, Fort Duquesne Bridge in Pennsylvania, using the LEFM approach, assuming no established AASHTO fatigue category for some of the details on this bridge.

In both of these approaches, determining the fatigue stress spectra is a crucial step which can significantly affect the fatigue life predictions. In general, there are two types of technique to obtain stress spectra, namely the model-based approaches and monitoring-based approaches. The traditional way of obtaining the fatigue stress spectra on bridges is generally based upon the stress analysis with a traffic load model and a structural model (Nyman & Moses 1985; Wang et al. 2005). In the modelling of traffic loads in the literature, three- and four-axle fatigue truck models are developed to represent actual trucks with axle number ranging from three to eleven collected by a weigh-in-motion (WIM) system (Szerszen et al. 1999; Miao & Chan 2002; Chotickai & Bowman 2006). It can be seen from these studies that the modelling of actual traffic loads is very complex, given the uncertainty associated with traffic parameters such as gross weights, axle weights, axle spacing and vehicle positions. Therefore, the accuracy of model-based approaches highly depends upon the rationality of traffic load models. In the study conducted by Battista et al. (2008), the volume of traffic was considered according to collected toll data and taken as constant for 2002 and forward from then. Average weights were assumed for all vehicles within each category and the load distributions between front and rear axles obtained from vehicle weighing data. In another study, Guo et al. (2012) represents the vehicles crossing the bridge during the measurement period with several random variables including the number of axles, axle weights, axle spacing and transverse position of vehicles and conducted probabilistic finite element analysis (FEA)

to consider the uncertainties in equivalent stress ranges and the number of stress cycles. Guo et al. (2015) identified mainly six types of vehicle crossing the Runyang Bridge, and the axle weights of most types of vehicle were described by a single-peak probability density function. However, for the last three types, a weighted sum of PDFs is used to describe such distributions due to the existence of multiple peaks in the PDFs. Yan et al. (2016) use Monte Carlo simulation to generate traffic loads in terms of axle weights and their corresponding transverse positions based on the traffic data monitored within one week over the Ningbo orthotropic bridge in China.

In this study, a 'scenario modelling' methodology is used to simulate site-specific traffic combinations derived from a Bridge Weigh-in-Motion (B-WIM) system. The simulated traffic is then used for the calculation of accumulated fatigue damage on the bridge at considered locations as a function of time. This is achieved by installing B-WIM sensors on the bridge and using them to record the traffic loading. Readings from other sensors are used to calibrate an FE model which, when combined with the calculated truck weights, is used to compute stresses throughout the entire bridge, including locations without any instrumentation. A fatigue damage accumulation model is developed to calculate fatigue damage at all points on the bridge – direct measurement points and virtually measured points. This provides bridge engineers with stress histories for every point, adding value to the SHM system. A summary of the virtual monitoring procedure implemented in the current study is shown in Figure 1. Given the extensive attempts at introducing different fatigue assessmnet frameworks shown in recent literature, the novelty of this work lies in the utilisation of WIM data to produce complex traffic scenarios which results in site-specific stress spectra for a longer period of time, and its application on an orthotropic cable-stayed bridge.

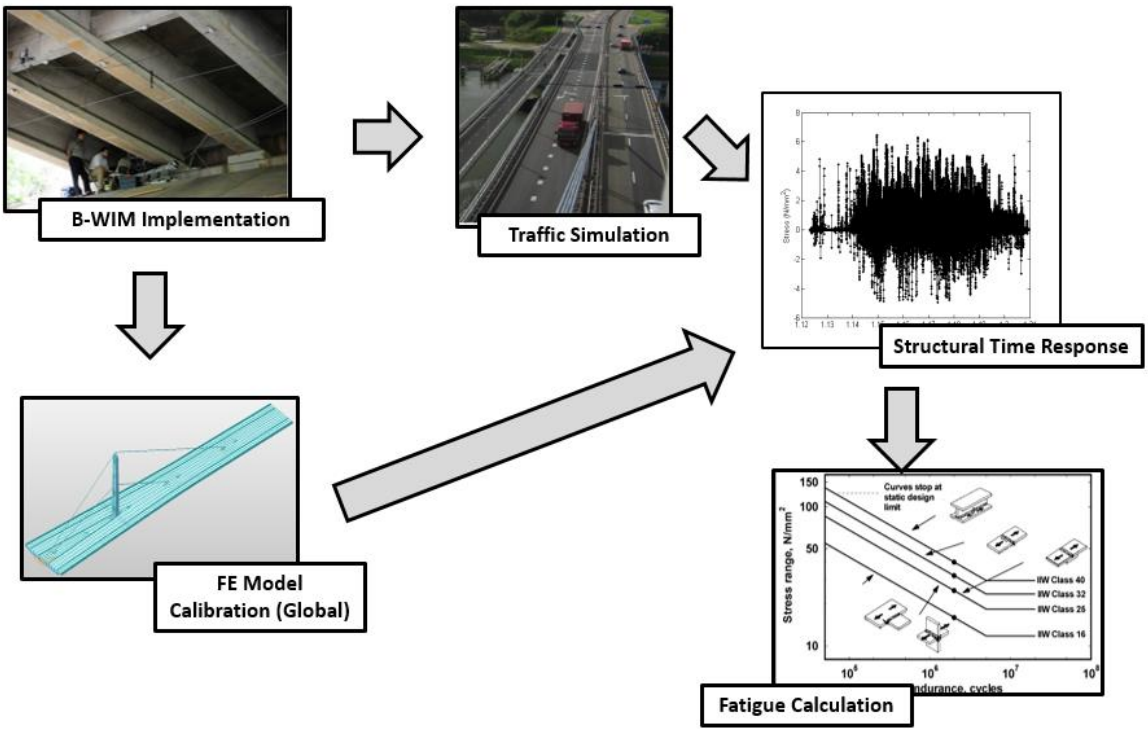

Figure 1: Virtual monitoring flowchart

For this research, a steel bridge in the Netherlands, designed and built in 1960's, is selected as a case study to develop the Virtual Monitoring concept and to examine the efficiency of the developed methodology. The bridge was instrumented with sensors which were used to (i) calculate the traffic loading and (ii) calibrate the FE model of the bridge. The combination of traffic information with the numerical model facilitated the identification of 'hotspot' locations on the bridge, where fatigue damage is expected to be a major concern. Based on these defined locations, the FE model is refined to simulate particular parts of the bridge in more detail. Based on the responses collected from sensors located in some of the aforementioned 'hotspots', the accuracy of the developed Virtual Monitoring software was assessed.

The selected case study is a steel bridge near the city of Rotterdam. It is a heavily trafficked structure with a large proportion of the vehicles being heavy trucks, moving goods to and

from the various harbours of the Europort complex, one of the busiest ports in the world. This bridge actually comprises three different structures (see Figure 2):

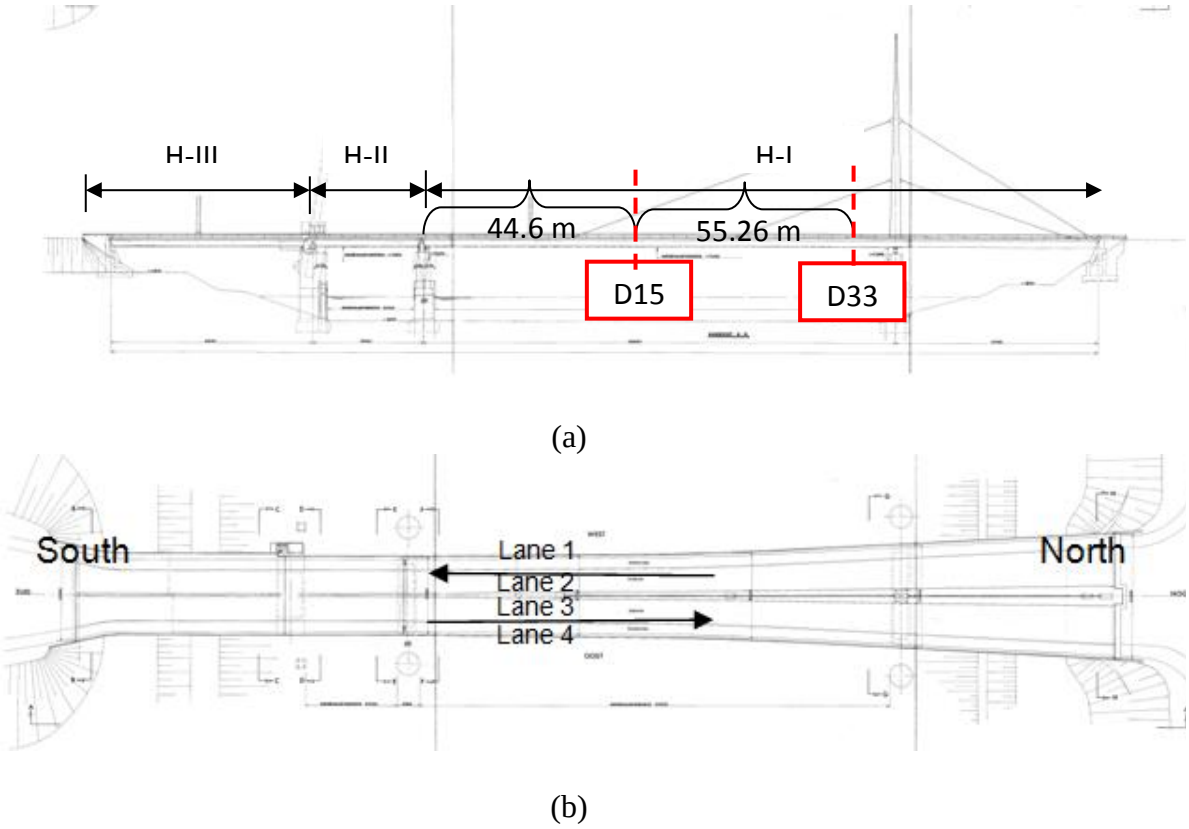

Figure 2: Individual codes for each structure and lane configuration of the steel bridge system: (a) Plan; (b) Elevation

- H-I: This target structure for monitoring is a cable-stayed orthotropic steel deck bridge (side span with a length of 47 m and a main span of 108 m).
- H-II: Draw bridge (movable structure) (span length 25.5m). This part of the bridge is not considered in the analysis and no measurements were taken on it.
- H-III: Steel girder with an orthotropic bridge deck (span length 46.5m). H-III is made up of two main load-carrying girders, 1.8 m deep, that span 46.5 m; 17 cross beams and an orthotropic deck. The deck's dimensions change near the southern abutment. Most of the bridge is 15.8 m wide but this gradually increases to 18.7 m in the last 8 m of the southern end.

Ideally, when installing a Virtual Monitoring system, the sensors installed on the bridge would serve the dual purpose of (i) calculating vehicle weights using a B-WIM algorithm and (ii) allowing calibration of the FE model of the bridge required for the implementation of Virtual Monitoring. Due to the structural complexity of the cable stayed bridge to be monitored (H-I), and the presence of a simply-supported bridge (H-III) directly adjacent to it, it was decided to install the B-WIM system separately on the simply-supported span (H-III). This decision was made to ensure the accuracy of the truck weights calculated by the B-WIM system. The simply-supported span is much more suitable for a typical B-WIM installation and carries the same traffic as the main bridge (H-I). As a result, an additional set of sensors was required on H-I to facilitate calibration of the FE model. Two sets of ST-503 sensors were installed for the B-WIM system on H-III: a set of 4 near the abutment for axle detection and a second set of 24 sensors as close to the central section as possible.

Using the commercial SiWIM® system (OBrien et al. 2008), B-WIM records were collected for 38 days from October 30th to December 7th, 2013. Each ST-503 strain transducer is equipped with 4 strain gauges in a full Wheatstone configuration. They measure strains, i.e. elongations of the structure between two anchor points placed approximately 200 mm apart. In this installation, the transducers are bolted into steel mounting plates bonded chemically to the surface of the bridge. The system continuously calculates signal offsets that arise primarily due to temperature effects, and zeroes them when the offset exceeds predefined thresholds (Žnidarič & Kalin, 2014). Measured signals were processed by the SiWIM SPU-23 processing module, designed around an embedded industrial personal computer running the Windows® operating system, an analogue to digital converter and a hard drive. The system was configured remotely through a wireless link.

The Bridge WIM software comprises 5 main independent components, coded for and operating in the 32-bit Microsoft Windows environment, namely: the Engine software calculating influence lines and storing raw and aggregated data on the vehicles; the Front End software adjusting weighing parameters (axle weights and gross weights of vehicles) and displaying the results; the Data Processing software post-processing and evaluating measured data; the Supervision software providing web-based checking, control and off-site analysis of the systems present and the Monitoring software used for pre-selection of illegally overloaded trucks. The SiWIM system calculates the influence lines for the bridge using selected vehicles, without knowing the actual axle loads and axle spacings, using a non-linear minimisation procedure that provides the best solution for individual vehicles (Žnidarič et al. 2011). A number of such evaluations (typically some tens) are then averaged into the influence lines that are used for further calculations. In the original Moses' algorithm (Moses, 1979) the unknowns are only the axle loads. In the Influence Line (IL) calculation algorithm, the IL itself is also an unknown. SiWIM uses Powell's minimisation to solve the problem.

In this study, for each vehicle, the Bridge WIM system recorded and analysed the following: date, time stamp, speed, lane, category (type of truck), Gross Vehicle Weight (GVW), individual axle weights, wheelbase and axle spacings. The resolution of the time stamps was 0.001 second and the scan rate for the transducers was 1000 Hz. The WIM data were checked for quality assurance purposes. Records with zero or negative GVW/axle weight (approximately 4%) were removed from the raw data. Trucks with one or no axles or trucks with a wheel base over 30 m were also removed from the recorded measurements. These errors are presumed to have occurred as a result of large dynamics in the recorded signals which made it difficult for the B-WIM system to detect axles travelling over the bridge. This

can be a problem for light vehicles on slender bridges. The full list of cleaning rules applied is documented in Enright and OBrien (2008). The cleaned data were processed to obtain detailed information on traffic travelling in each lane. The lane configuration and numbering is given in Figure 2. Results confirm that lanes 1 and 4 are the slow lanes in each direction, with higher average GVW, as expected.

A set of sensors were installed in H-I to allow the calibration/validation of the developed FE model of the global response of the structure. The sensors were located at sections that feature predominantly global effects. Strain gauges were placed inside the pylon to record strains in the longitudinal and transverse direction. The information provided by these sensors was used to validate the global model. A total of 24 sensors were located on the main deck where the load effects due to passing vehicles were expected to be important (i.e., hotspot locations). The influence of local effects such as changes in plate thickness and the pylon-to-deck connection were taken into consideration in the FE model.

Based on preliminary results using the developed model and local effect considerations, the sensors were installed at H-I D15 and H-I D33 as shown in Figure 2. Sensors were installed directly on the plate between the stiffeners, oriented parallel to the stiffeners (Figure 3). Measurements collected from strain gauges are in the form of voltages and were converted to micro strain using the manufacture's gauge factor.

a)

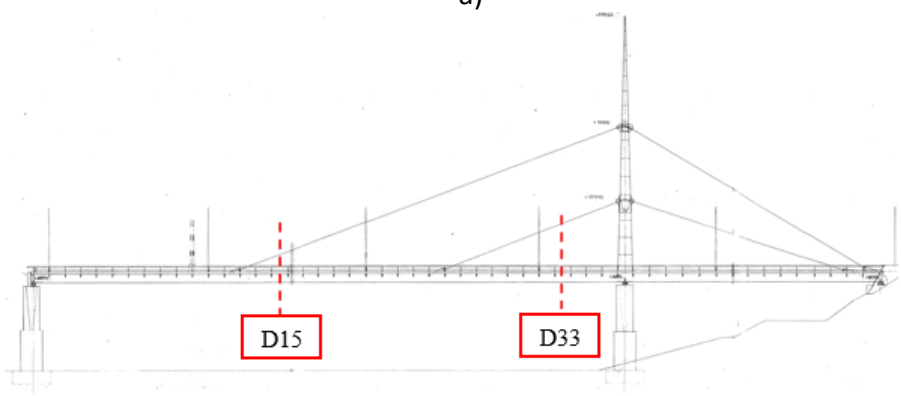

b)

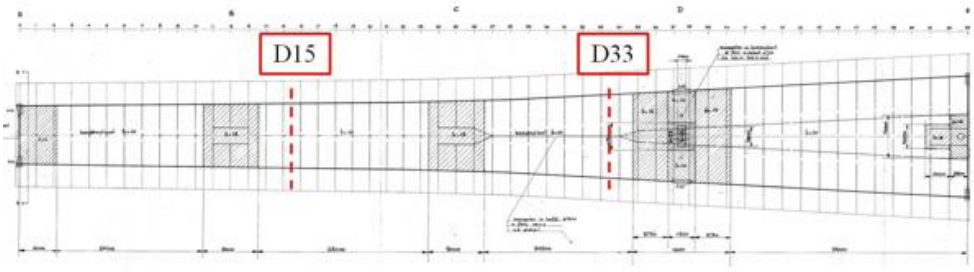

c)

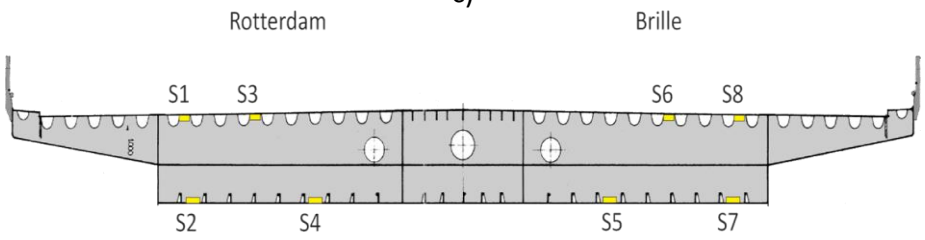

d)

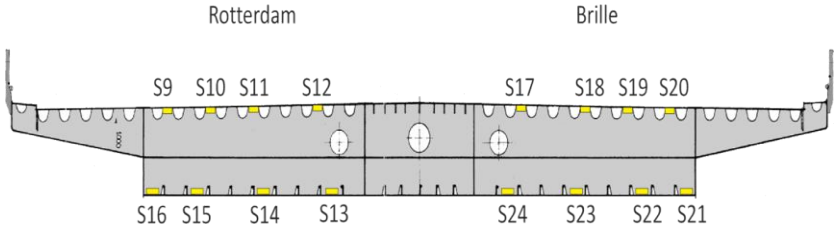

e)

Figure 3: a) Example of instrumented strain gauges, b) Main deck sections (side view), c) Main deck sections (top view), d) Strain gauges configuration at D15, e) Strain gauges configuration at D33

Strains on all channels exhibited a significant drift from the baseline. This was removed with a low pass filter. Measurements from each channel were divided into 0.25 second long segments and checked to ensure that the variation in voltages was within 0.02 volts. Each signal segment was saved in an event file. The average voltage for each event file and each channel was offset (subtracted) from the signal during a post-processing procedure. One of the drawbacks of using this offset correction is the inconsistency in offset values for each event file - each offset is different. This results in differences in adjacent signal segments from consecutive event files. For example, Figure 4 shows three consecutive event files in three different colours. The steps between the signal segments are due to different offsets removed from each event file. The gap in the consecutive event files was removed by deducting the difference between signals in the overlapping segments. The time overlap between stresses in the event files is due to the definition of entry time of each event in the software.

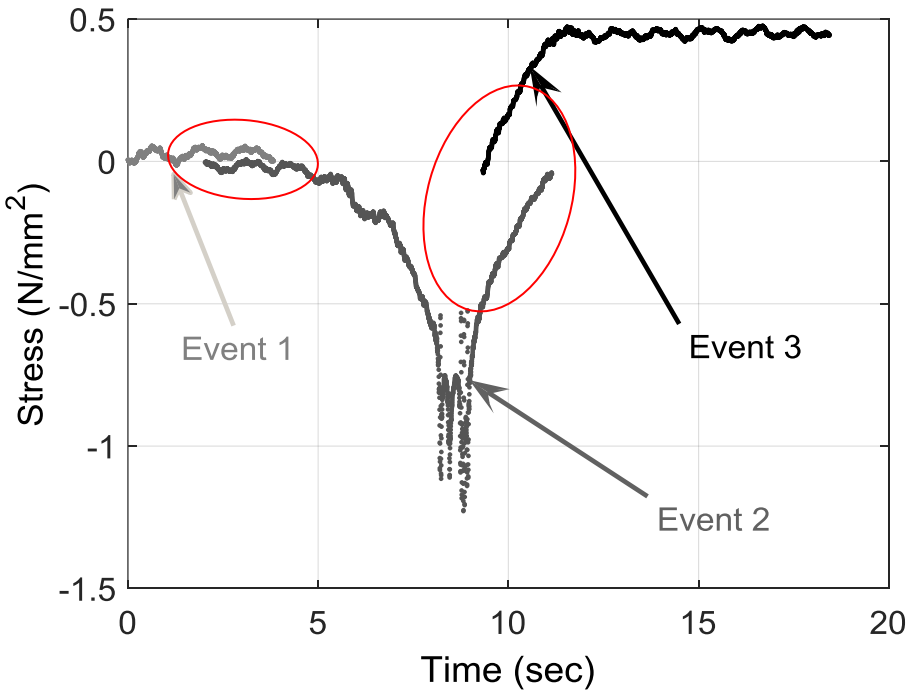

Figure 4: Example of recorded signals in consecutive event files

Finite element model

An FE model of the cable-stayed part of structure H-I was developed using the software, Midas Civil. The objective was to accurately describe the global response of the bridge which would subsequently be calibrated and validated via recorded measurements. The model dimensions and properties were chosen based on those measured or indicated in drawings of the bridge.

Only static calculations in the linear-elastic range were performed in this study. Three main load types were considered: dead load, cable tensions and moving traffic loads. In particular, the moving load analysis calculated the static bridge response for a load located at any position on the deck. With this information the unit influence surface for any load effect and at any location could be obtained. Figure 5 presents a general view of the developed FE model, built as a combination of truss, beam and plate elements. The model is made up of 3267 nodes and 5959 elements.

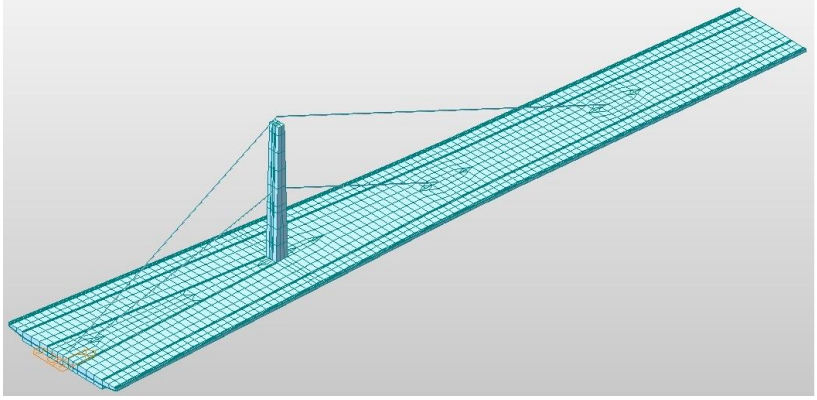

Figure 5: Isometric view of FE model of full cable-stayed (H-I) bridge

According to the drawings, two grades of steel were used in the construction, namely S235 and S355, both with Elastic Modulus of 210×10^3 N/mm^2, Poisson's ratio of 0.3 and weight

density of 76.98×10^3 N/m^3. The only difference between these steel grades is in their yield strengths which has no influence on the analysis. The cables are made of steel and the Young's modulus has been adjusted to 165 kN/mm^2 to account for the change in stiffness due to the sag caused by self-weight of the cables. Other materials, such as asphalt and concrete kentledge were treated as surface loads. The main deck is a complex orthotropic steel structure with variable dimensions along the longitudinal axis. It was modelled using a combination of beam and plate elements.

Finite Element Model Calibration

The FE model was calibrated to correctly describe the global response of the bridge. This was performed in an iterative manner by adjusting the model parameters (e.g. material properties) until the results approximated well to the available recorded information. First the measured cable tensions determined in a previous study by TNO (Nederlandse Organisatie voor Toegepast Natuurwetenschappelijk Onderzoek) were compared to the calculated cable tensions in the FE model, taking into account the self-weight and imposed loads (Table 1). Two conditions were considered for cable supports. In the first case (i.e., Cable Control 1), it was assumed that the cable forces are different in cables 3 and 4 (two cables over lower saddle). In the second case (Cable Control 2) the cable forces were assumed to be identical for cables 3 and 4. The first case gave results in better agreement with the TNO values (Table 2). The sensitivity of cable forces to the elastic modulus of the deck and cables was also examined and it was found that the assumed elastic modules in the model (210 GPa for deck and 165 GPa for cables) were optimum, i.e., these resulted in minimum difference from the TNO values.

Table 1: Cable Forces Measured by TNO and obtained in FE model

	TNO	Cable Control 1	Cable Control 2
Cable 1	10079	10652.912	10653.036
Cable 2	9362	9486.008	9485.424
Cable 3	8880	8191.451	8423.621
Cable 4	9143	8694.177	8432.621

Table2: Error in Cable forces obtained from FE model

Error %			
	TNO	Cable Control 1	Cable Control 2
Cable 1	------	5.69	5.70
Cable 2	------	1.32	1.32
Cable 3	------	7.75	5.14
Cable 4	------	4.91	7.77
Average		4.92	4.98

In the next stage of validation, the model was fine-tuned to match the measured strain records at various locations on the bridge. Traffic information collected by the B-WIM sensors was used with influence lines for each sensor, determined from the FE model, to obtain stress histories for each channel. These were then compared to the measured strain histories. In this process, the difference between measurements and the FE model was minimised by varying the boundary conditions, element size, stiffener modelling, cable to deck connections (using rigid links), saddle details (fixed to the pylon using rigid links for upper saddle and

articulated using a beam element and a hinge for lower saddle) and asphalt layer modelling. This process has not affected the calculate cable tensions in the previous step.

It was found that three nodes with restraint in vertical translation is the best representation of the two elastic bearings and one vertical translational support at the south abutment. As for the pylon, the supports have particularly large contact areas and the deck near these supports has been stiffened with additional plates. To account for that, the boundary conditions in the FEM consist of two nodes restrained in the longitudinal direction. For the supports at the edges, the nodes have been restrained in the vertical direction only. For the central support, translation in all three coordinate directions are fixed allowing only rotations. Finally, for the north abutment, the bearings are restrained in vertical translation at the corner nodes.

It was assumed that vehicles were travelling at the mid-path of each lane. In order to validate this assumption, the sensitivity to transverse load position was investigated by varying the transverse position of load in the FE model. The sensitivity analysis showed that the variation in stress at sensor 20 (located at D33) due to transverse variation of a single axle load within each lane is negligible. Consequently, it was assumed that the axles were travelling on the mid-path of each lane. A similar result was found for bending moment.

For sensor 20, Figure 6.(a) illustrates the comparison of stresses derived from numerical simulation to the corresponding measured stresses, for a few events on the 9^{th} day of measurement. The measured stresses correspond to three loading events and the simulations are due to traffic recorded in six event files (black dots on Figure 6.(a)). The time difference between simulation and measured stress can be explained by i) lack of synchronization

between the two measurement systems and ii) the difference between the assumed constant speed and the likely varying speed in the actual loading.

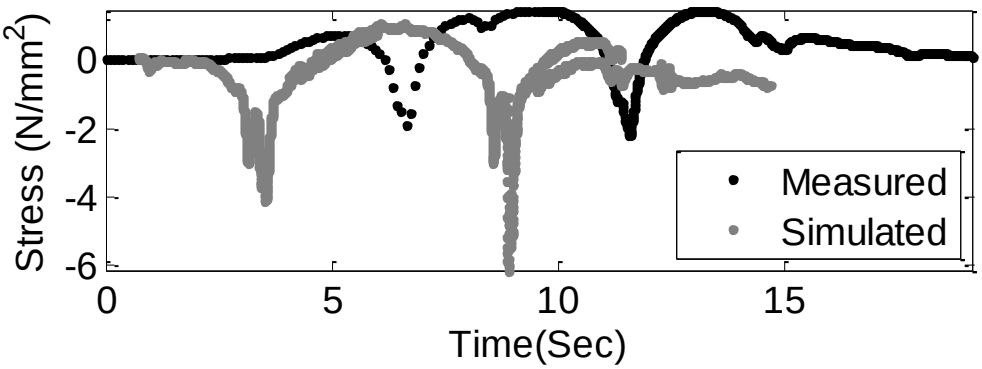

(a)

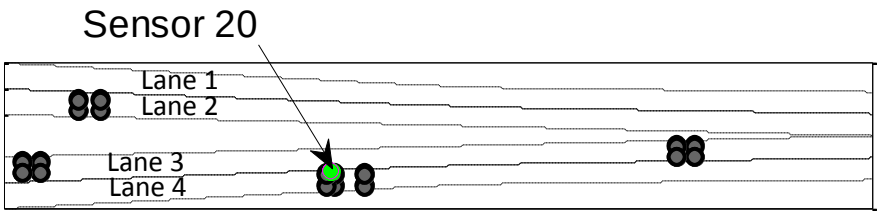

(b)

Figure 6: a) Response at Sensor 20 due to travelling traffic, b) load positions for maximum stress at sensor 20

In addition to the time difference, there is a difference in stress which is considered to be primarily due to the offsets in recorded strains and to local effects at the strain gauges (i.e., strain gauges show higher sensitivity to load position that found in the numerical model). Figure 6.(b) shows the vehicle positions corresponding to the maximum strain calculated at sensor 20. As can be seen from the figure, the maximum strain is due to a 3-axle truck on lane 4, two 2-axle trucks on lane 3 and a 2-axle truck on lane 2. As expected the peak load effect occurred when a heavy truck was located over the sensor.

Figure 7 illustrates stresses due to all the records on the 11th day. It can be seen from the figure that stress due to simulated traffic has more positive values than the measurements. This can be explained by the offsetting software which resulted in a shift towards negative stresses.

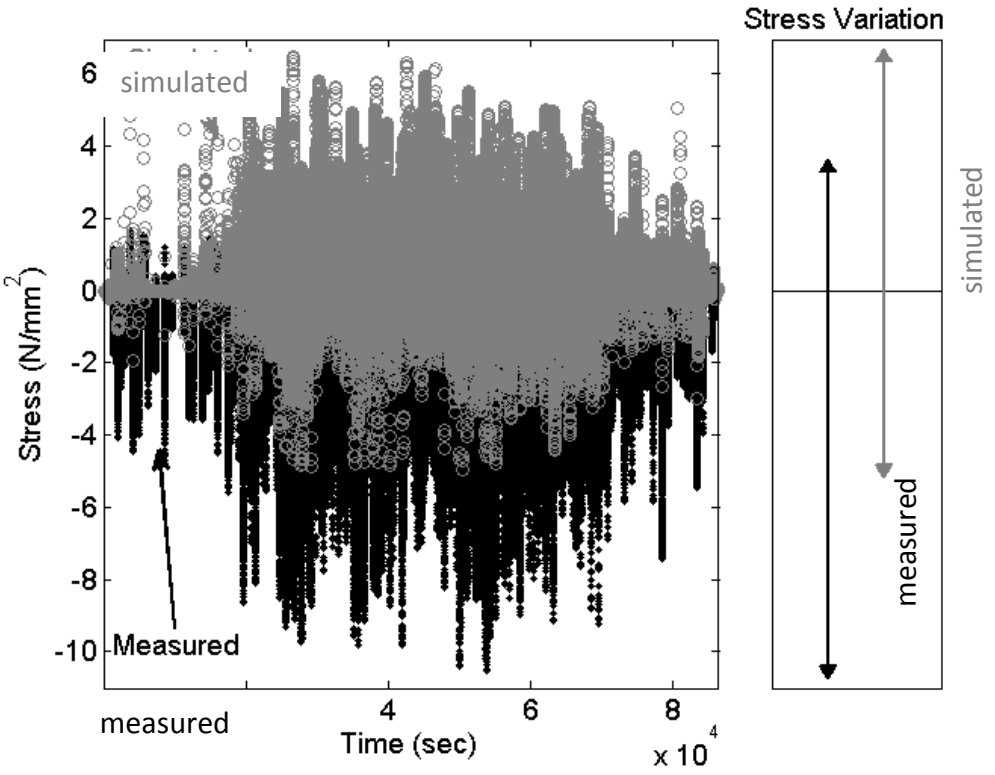

Figure 7: Measured and Simulated Stress at Sensor 20 for a Day of traffic

The purpose of the FE model calibration is to facilitate a more accurate fatigue life estimation. In order to carry out a fatigue damage calculation, a technique must be employed which can be used to count the number of times that the detail under consideration is subjected to different stress levels. Once the number of stress oscillations in each stress range has been evaluated, the fatigue damage calculation can be carried out using the appropriate *S-N* curve.

One of the preferred methods of dealing with stress cycles is the Rainflow counting method due to its simplicity, accuracy and computational efficiency (Socie et al. 1979). All counting methods require the turning points to be extracted from the signal. For example, in the given time response of Figure 5, the turning points for the small sample of stress history are shown in Figure 6. As expected, the number of turning points in the signal is significantly less than the number of signal records.

Rainflow cycle counting is a procedure for calculating damage due to variable amplitude loading. It was initially proposed by Matsuishi & Endo (1968) to count the cycles or the half cycles of strain-time signals. Rainflow cycle counting theory depends on the hysteresis loops in stress-strain behaviour (Socie et al. 1979). For a sufficiently long record, each valley-generated half-cycle will match a peak-generated half-cycle to form a whole cycle. The counting of peaks makes it possible to construct a histogram of the peaks of the random stress which can then be transformed into a stress spectrum, giving the number of events lower than a given stress value. By summing up the frequencies for each stress range amplitude, the variable stress cycles can be converted into a stress histogram.

Figure 8 shows the stress range histogram for sensor 20. While there are differences between measurements and simulations for individual events, this figure shows a very good match in probability/frequency, for each stress range. Clearly the offset effect evident in Figure 4 and Figure 5 does not influence the stress range histogram.

Results from other sensors located at D33 also show good agreement (less than 10% error) between simulated and measured stress histograms. Similar results were found for sensors located in the pylon.

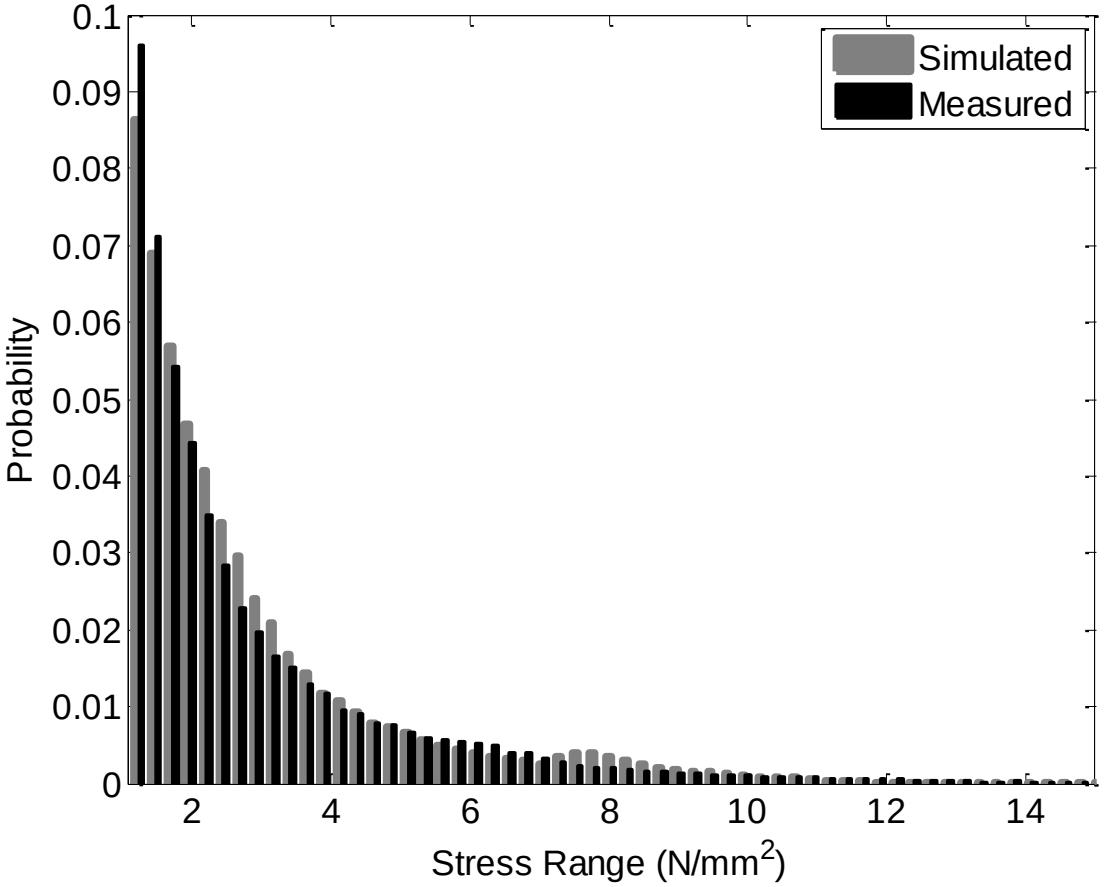

Figure 8: Measured and Simulated stress range histogram for a typical day of traffic data, for Sensor 20

It is concluded that the validated finite element model can be used for fatigue assessment with the simulated traffic.

Scenario Modelling Traffic Simulation

For fatigue assessment it was necessary to consider traffic for a duration much longer than the performed measurements which required a process of Monte Carlo simulation. Monte Carlo simulation of traffic, with each lane being simulated independently, was used for characteristic load effect estimation in the background studies during development of the EuroCode bridge load model (EC1, 2003). Although extrapolating load effects calculated from measured traffic implicitly incorporates the patterns of correlation in the traffic, it suffers

from relatively small quantities of data and high uncertainty due to the extrapolation process. Gindy and Nassif (2006) report up to 33% variation in results from extrapolation, and Dawe (2003) notes up to 20% variation for the characteristic load effect estimated from the EuroCode.

OBrien and Enright (2011) propose a method for modelling multi-lane same-direction traffic and show that the significant weight and gap correlations identified in extensive WIM data are modelled appropriately. In the simulation process, a form of smoothed bootstrap is applied, in which randomness is added to measured traffic scenarios by using Kernel Density functions. The subtle patterns of correlation and interdependence between vehicles weights, speeds and inter-vehicle gaps, which are evident in measured traffic, are reproduced in the simulation, and an element of randomness is added to vary the parameters. In bootstrapping, random samples are drawn repeatedly from the observed data. Here, the samples are traffic scenarios which consist of five to eight slow-lane trucks in succession, with any adjacent fast-lane trucks that are present in the second lane. Scenarios include all the properties of weight, axle configuration and relative vehicle positions. Prior to the simulation, all such scenarios are identified in the measured traffic.

In this study the scenarios are stitched together to generate multi-lane streams of traffic. Each scenario is selected randomly from all scenarios corresponding to the flow rate for the time of day. In this way, the measured relative frequencies of the parameters of scenarios (i.e., GVW, gaps and flow rate) are reproduced in the simulation. To increase the variability in the scenarios, random 'noise' is applied using variable-bandwidth Kernel functions. Kernel functions are used to modify the GVWs and gaps in a scenario each time it is selected. Once all vehicles in a selected scenario have been generated, the scenario is added to the simulated

traffic stream, and the next scenario is selected from the data. Detailed discussion on the kernel functions and bandwidths used are given elsewhere (OBrien and Enright 2011). Bridge load effects are calculated for the traffic stream using appropriate influence lines.

In this study, 15 years of traffic is simulated using scenarios taken from 40 days of measured traffic. The GVW and gaps are perturbed using truncated Normal and triangular Kernel Density functions, respectively. In order to validate the procedure, load effects resulting from 40 days of simulated traffic are compared to the 40 days of measured traffic. The cumulative probability distributions of load effects due to measured and simulated traffic are illustrated in Figure 9. The vertical axis in this figure is probability of non-exceedance, plotted to a Gumbel scale (double log scale of cumulative distribution function, i.e., -log(-log(p)), where p is the probability of non-exceedance). This rescaling of the vertical axis allows the trends in the extreme tail of the data to be examined more clearly. For this figure, bending moment at mid-span for a simply supported beam is calculated for simulated and measured traffic. As can be seen in Figure 9, good agreement between the distributions validates the methodology used for simulated traffic (i.e., less than 1% error in general trend and less than 4% error in 50-year characteristic value).

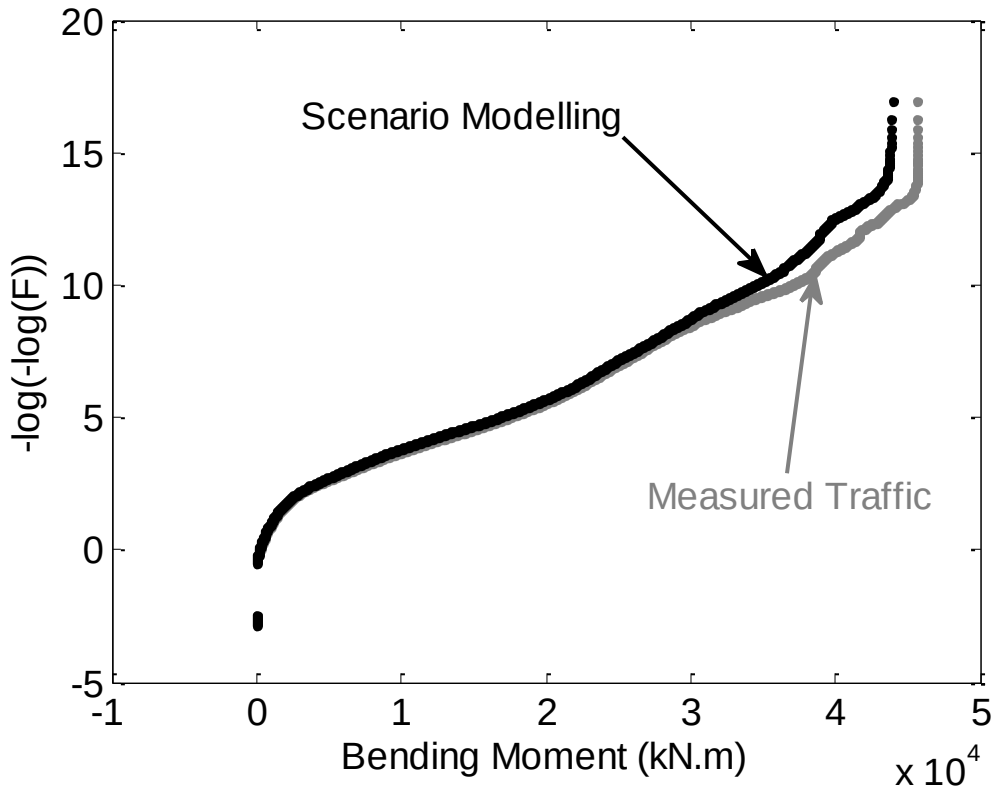

Figure 9: CDF of Bending Moment (maximum per loading event) at Mid-span of simply supported beam due to simulated and measured traffic (F=probability of non-exceedance)

Fatigue Assessment of the Steel Bridge

Figure 10.(a) shows the stress spectrum for sensor 20 due to 15 years of simulated traffic. The maximum stress range is 17.9 N/mm^2 with 100 such cycles in 15 years. In this spectrum any stress range below 1 N/mm^2 is neglected.

The EuroCode load model 1 is also applied to the influence lines derived from the FE model. Fatigue Load Model 1 has the configuration of the characteristic Load Model 1 defined in EC 1991-2 (EC1, 2003) with the values of the axle loads equal to $0.7Q_{ik}$ and the values of the uniformly distributed loads equal to $0.3q_{ik}$ and $0.3q_{rk}$. $Q_{ik}$is the characteristic axle load (Load Model 1) on notional lane number i , q_{ik} is the characteristic distributed load and q_{rk} is the characteristic distributed load on the remaining area of the carriageway outside the notional lane. In this comparison two categories are chosen: Category 90 and Category 112 from the

Eurocode. As can be seen the maximum stress range at this location does not exceed the limit in either category; consequently, damage is zero due for both load models.

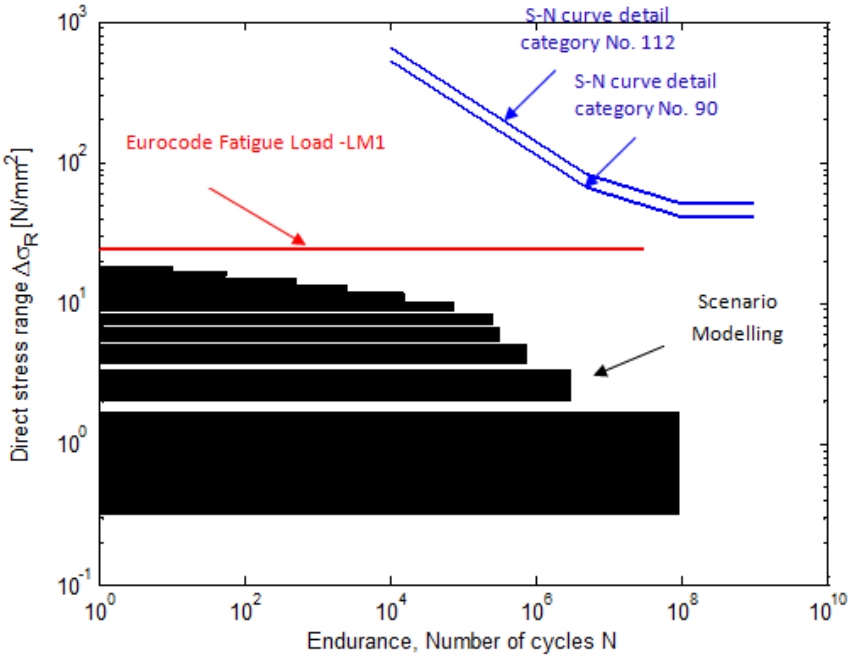

(a). sensor 20 at D33

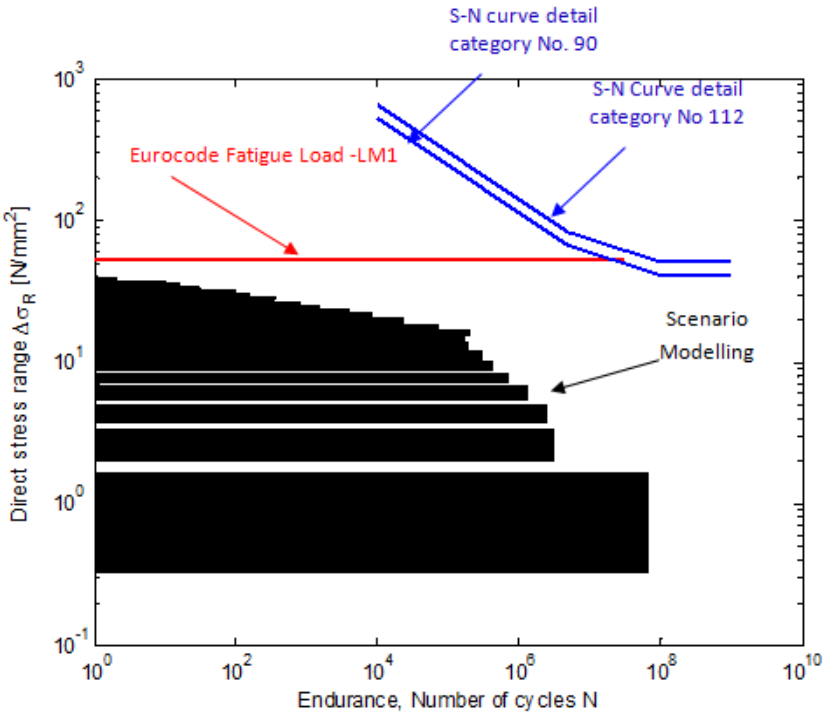

(b). sensor 8 at D15

Figure 10: Stress Spectrum due to scenario modelling and EC FLM1 for 15 years

Influence lines obtained from the numerical model show that generally sensors located at D15 illustrate higher stresses in comparison to stresses at D33. This suggests that the accumulated damage needs to be also checked for a sensor at D15. Sensor 8 is chosen for this purpose. Figure 10.(b) shows the comparison between both the EC generated stress ranges and the scenario modelling stress spectrum for the same categories used in the D33 check. It is evident from the figure that the Eurocode generated stress range exceeds the limit in both categories. For the stress ranges derived from Scenario Modelling, on the other hand there is considerable reserve capacity. This is an important finding as it shows that, despite it being a heavily trafficked site, the stress range spectrum is still considerably less that than specified in the Eurocode.

It should be noted that the traffic simulated using scenario modelling does not take account of dynamic and congestion events for which the stress level may be higher.

Conclusion

This paper presents a framework for Virtual Monitoring of steel bridges which allows the virtual monitoring of a bridge at locations where there are no sensors. The application of Virtual Monitoring to a fatigue damage calculation is outlined for a cable stayed steel bridge in the Netherlands. This bridge was instrumented using two sets of sensors: (i) a B-WIM system for calculating vehicle weights and (ii) an additional set of sensors which were used to calibrate the FE model. Results from sensors on the pylon and the right hand side at D33 gives a good match between measured and simulated stresses.

Based on traffic information derived from 40 days of measurements, 15 years of traffic is simulated using Scenario Modelling. As expected the EuroCode model is found to be conservative. Virtual monitoring has obvious potential to facilitate maintenance optimization and lifecycle cost reductions through the avoidance of unnecessary repair and/or replacement of serviceable bridge structures. Overall the study suggests that the developed SHM system is capable of greatly reducing the conservatism involved in methods often currently used in practice.

Acknowledgement

This work was supported through the BridgeMon project. BridgeMon was funded by the European Commission 7th Framework Programme (grant agreement n°315629). The authors acknowledge the Dutch Ministry of Transport and Infrastructure, Rijkswaterstaat, for their cooperation and support. The authors also gratefully acknowledge the contributions of the

other BridgeMon consortium partners: CESTEL CESTNI INZENIRING DOO, KALIBRA INVESTMENTS BV, ADAPTRONICA ZOO SP, ZAVOD ZA GRADBENISTVO SLOVENIJE (ZAG) and CORNER STONE INTERNATIONAL SAGL

References

Alampalli, S. 2012. Special Issue on Nondestructive Evaluation and Testing for Bridge Inspection and Evaluation. Journal of Bridge Engineering, 17(6), pp.827–828.

AASHTO. 2010. LRFD Bridge Design Specifications. 5th ed., Washington D.C.: American Association of State Highway and Transportation Officials.

Battista, R.C., Pfeil, M.S. & Carvalho, E.M.L. 2008. Fatigue life estimates for a slender orthotropic steel deck. Journal of Constructional Steel Research, 64(1), pp.134–143.

Canadian Infrastructure. 2016. Canadian infrastructure report card - informing the future, Available at: http://www.canadainfrastructure.ca/downloads/Canadian_Infrastructure_Report_2016.pdf#page=28 [Accessed October 2, 2016].

Canadian Institute of Steel Construction. 2007. Handbook of steel construction 9th Edition.

Chellini, G., Lippi, F.V. & Salvatore, W. 2014. A multidisciplinary approach for fatigue assessment of a steel–concrete high-speed railway bridge on Sesia river. Structure and Infrastructure Engineering, 10(2), pp.189–212.

Cheung, M. S., Tadros, G. S., Brown, T., Dilger, W. H., Ghali, A. & Lau, D. T. 1997. Field monitoring and research on performance of the Confederation Bridge. Canadian Journal of Civil Engineering, 24(6), pp.951–962.

Cohen, H., Fu, G., Dekelbab, W., & Moses, F. 2003. Predicting truck load spectra under weight limit changes and its application to steel bridge fatigue assessment. Journal of Bridge Engineering, 8(5), 312-322.

Chotickai, P. & Bowman, M.D. 2006. Truck models for improved fatigue life predictions of steel bridges. Journal of Bridge Engineering, 11(1), pp.71–80.

Chryssanthopoulos, M.K. & Righiniotis, T.D. 2006. Fatigue reliability of welded steel structures. Journal of Constructional Steel Research, 62(11), pp.1199–1209.

Clarke, J.N., 2014. Investigating the remaining fatigue reliability of an aging orthotropic steel plate deck. Dalhousie University.

Cross, E.J. Koo, K.J., Brownjohn, J.M.W. & Worden, K. 2013. Long-term monitoring and data analysis of the Tamar Bridge. Mechanical Systems and Signal Processing, 35, pp.16–34.

Dawe, P. 2003. Research Perspectives: Traffic loading on highway bridges. London, United Kingdom: Thomas Telford.

Desjardins, S. L., Londoño, N. A., Lau, D. T. & Khoo, H. 2006. Real-Time data processing, analysis and visualization for structural monitoring of the confederation bridge. Advances in Structural Engineering, 9(1), pp.141–157.

Dudás, K., Jakab, G., Kövesdi, B. & Dunai, L. 2015. Assessment of fatigue behaviour of orthotropic steel bridge decks using monitoring system. Procedia Engineering, 133, pp.770–777.

EC1. 2003. Eurocode 1: Actions on structures, Part 2: Traffic loads on bridges. European Standard EN 1991-2:2003, Brussels: European Committee for Standardization.

EC3. 2005. Eurocode 3: Design of steel structures, Parts 1-9: Fatigue strength of steel structures, European Standard EN 1993-1-9.

Enright, B. & OBrien, E.J. 2011. Cleaning Weigh-in-Motion data: techniques and recommendations, University College Dublin and Dublin Institute of Technology, Viewed 3rd September, 2013.

Farreras-Alcover, I., Chryssanthopoulos, M.K. & Andersen, J.E., 2016. Data-based models for fatigue reliability of orthotropic steel bridge decks based on temperature, traffic and strain monitoring. International Journal of Fatigue, http://dx.doi.org/10.1016/j.ijfatigue.2016.09.019.

Frangopol, D.M. 2011. Life-cycle performance, management, and optimisation of structural systems under uncertainty: accomplishments and challenges. Structure and Infrastructure Engineering, 7(6), pp.389–413

Frangopol, D.M. Strauss, A. & Kim, S., 2008. Bridge reliability assessment based on monitoring. Journal of Bridge Engineering, 13(3), pp.258–270.

Ge, Y. & Xiang, H. 2011. Concept and requirements of sustainable development in bridge engineering. Frontiers of Architecture and Civil Engineering in China, 5(4), pp.432–450.

Ghodoosipoor, F. 2013. Development of deterioration models for bridge decks using system reliability analysis. PhD Thesis, Concordia University, Montréal, Québec, Canada.

Gindy M., Nassif H.H. 2006. Comparison of traffic load models based on simulation and measured data. Joint International Conference on Coputing and Decision Making in Civil and Building Engineering. Montreal, Canada, 2497-506.Guo, T. & Chen, Y.W., 2011. Field stress/displacement monitoring and fatigue reliability assessment of retrofitted steel bridge details. Engineering Failure Analysis, 18(1), pp.354–363.

Guo, T. & Chen, Y.-W. 2013. Fatigue reliability analysis of steel bridge details based on field-monitored data and linear elastic fracture mechanics. Structure and Infrastructure Engineering, 9(5), pp.496–505

Guo, T., Frangopol, D.M. & Chen, Y. 2012. Fatigue reliability assessment of steel bridge details integrating weigh-in-motion data and probabilistic finite element analysis. Computers and Structures, 112–113, pp.245–257.

Guo, T., Liu, Z.-X. & Zhu, J. 2015. Fatigue reliability assessment of orthotropic steel bridge decks based on probabilistic multi-scale finite element analysis. Advanced Steel Construction, 11(3), pp.334–346.

Guo Tong, T., Li Aiqun, A. & Li Jianhui, J. 2008. Fatigue life prediction of welded joints in orthotropic steel decks considering temperature effect and increasing traffic flow. Structural Health Monitoring, 7(3), pp.189–202.

Hammad, A., Yan, J. & Mostofi, B. 2007. Recent development of bridge management systems in Canada. In Annual Conference of the Transportation Association of Canada. Saskatoon, Saskatchewan, Canada.

Inaudi, D. 2010. Overview of 40 bridge structural health monitoring projects. In International Bridge Conference, IBC 09-45.

Kim, S.H., Lee, S.W. & Mha, H.S. 2001. Fatigue reliability assessment of an existing steel railroad bridge. Engineering Structures, 23(10), pp.1203–1211.

Kolstein, M.H. 2007. Fatigue classification of welded joints in orthotropic steel bridge decks | TU Delft Repositories. Department of Civil Engineering and Geosciences, Delft University of Technology, TU-Delft.

Kwon, K. & Frangopol, D.M. 2010. Bridge fatigue reliability assessment using probability density functions of equivalent stress range based on field monitoring data. International Journal of Fatigue, 32, pp.1221–1232.

Leander, J., Andersson, A. & Karoumi, R. 2010. Monitoring and enhanced fatigue evaluation of a steel railway bridge. Engineering Structures, 32(3), pp.854–863

Lee, Y.J. & Cho, S. 2016. SHM-based probabilistic fatigue life prediction for bridges based on fe model updating. Sensors (Switzerland), 16(3).

Liu, M., Frangopol, D.M. & Kwon, K. 2010. Fatigue reliability assessment of retrofitted steel bridges integrating monitored data. Structural Safety, 32(1), pp.77–89.

Lovejoy, S.C. 2003. Determining appropriate fatigue inspection intervals for steel bridge members. Journal of Bridge Engineering, 8(2), 66-72. Lu, N., Noori, M. & Liu, Y., 2016. Fatigue reliability assessment of welded steel bridge Decks under stochastic fatigue truck loads via Machine Learning. Journal of Bridge Engineering, American Society of Civil Engineers, pp.1–12.

Mahmoud, H.N., Hodgson, I.C. & Bowman, C.A. 2006. Instrumentation, field testing, and fatigue evaluation of selected approach spans of the Throgs Neck bridge (TN82) over the East River, New York.

Massarelli, P.J. & Baber, T.T. 2001. Final report on fatigue reliability of steel highway bridge details. In Cooperation with the U.S. Department of Transportation Federal Highway Administration. Charlottesville, Virginia Virginia Transportation Research Council.

Matsuishi, M., and Endo, T. 1968. Fatigue of metals subjected to varying stress. Paper presented to Japan Society of Mechanical Engineers, Fukuoka, Japan. 37-40.Messervey, T.B., Frangopol, D.M. & Casciati, S., 2011. Application of the statistics of extremes to the reliability assessment and performance prediction of monitored highway bridges. Structure and Infrastructure Engineering, 7(1–2), pp.87–99.

Miao, T.J. & Chan, T.H.T. 2002. Bridge live load models from WIM data. Engineering Structures, 24(8), pp.1071–1084.

Miner, M.A., 1945. Cumulative damage in fatigue Journal of Applied Mechanics. Journal of Applied Mechanics.

Moses, F. 1979. Weigh-In-Motion system using instrumented bridges. ASCE Transportation Engineering Journal, 105: 233-249.

Mufti, A.A. 2002. Structural health monitoring of innovative Canadian civil engineering structures. Structural Health Monitoring, 1(1), pp.89–103.

Newhook, J.P. & Edalatmanesh, R. 2013. Integrating reliability and structural health monitoring in the fatigue assessment of concrete bridge decks. Structure and Infrastructure Engineering: Maintenance, Management, Life-Cycle Design and Performance, 9(7), pp.619–633.

Ni, Y.Q., Ye, X.W. & Ko, J.M. 2010. Monitoring-based fatigue reliability assessment of steel bridges: analytical model and application. Journal of Structural Engineering, 136(12), pp.1563–1573.

Nyman, W.E. & Moses, F. 1985. Calibration of bridge fatigue design model. Journal of Structural Engineering, 111(6), pp.1251–1266.

OBrien, E.J., Znidaric, A & Ojio, T. 2008. Bridge-Weigh-in-Motion – latest developments and applications world-wide. International Conference of Heavy Vehicles - ICWIM5, Paris, France, 2008, pp. 39-56.

OBrien E.J. and Enright B. 2011. Modeling same-direction two-lane traffic for bridge loading. Structural Safety. 33,296-304.Okasha, N.M., Frangopol, D.M. & Orcesi, A.D., 2012. Automated finite element updating using strain data for the lifetime reliability assessment of bridges. Reliability Engineering and System Safety, 99, pp.139–150.

Orcesi, A.D. & Frangopol, D.M. 2013. Bridge performance monitoring based on traffic data. Journal of Engineering Mechanics, 139(11), pp.1508–1520.

Saberi, M.R. et al. 2016. Bridge fatigue service-life estimation using operational strain measurements. Journal of Bridge Engineering, American Society of Civil Engineers, p.4016005.

Sakagami, T. 2015. Remote non-destructive evaluation technique using infrared thermography for fatigue cracks in steel bridges. Fatigue & Fracture of Engineering Materials & Structures, 38(7), pp.755–779.

Socie, D., Shifflet, G., and Burns, H. 1979. A field recording system with applications to fatique analysis. International Journal of Fatigue, 1(2), 103-111.

Szerszen, M.M., Nowak, A.S. & Laman, J.A. 1999. Fatigue reliability of steel bridges. Journal of Constructional Steel Research, 52(1), pp.83–92.

Wang, T.-L., Liu, C., Huang, D. & Shahawy, M. 2005. Truck loading and fatigue damage analysis for girder bridges based on Weigh-in-Motion data. Journal of Bridge Engineering, 10(1), pp.12–20.

Wang, Y., Li, Z.X. & Li, A.Q. 2010. Combined use of SHMS and finite element strain data for assessing the fatigue reliability index of girder components in long-span cable-stayed bridge. Theoretical and Applied Fracture Mechanics, 54(2), pp.127–136.

Watanabe, E., Furuta, H., Yamaguchi, T. & Kano, M. 2014. On longevity and monitoring technologies of bridges: a survey study by the Japanese Society of Steel Construction. Structure and Infrastructure Engineering, 10(4), pp.471–491.

Yan, F., Chen, W. & Lin, Z. 2016. Prediction of fatigue life of welded details in cable-stayed orthotropic steel deck bridges. Engineering Structures, 127, pp.344–358.

Ye, X., Su, Y. & Han, J. 2014. A State-of-the-art review on fatigue life assessment of steel bridges. Mathematical Problems in Engineering, Hindawi Publishing Corporation, pp.1–13.

Žnidarič, A. & Kalin, J. 2014. Technical specifications for optimised Bridge WIM axle detection. Deliverable D1.4, EU funded BridgeMon project (Bridge Monitoring), 2012 - 2014, GA no. 315629.Žnidarič, A., Lavrič, I., Kalin, J., & Kulauzović, B. (2011). *SiWIM Bridge Wiegh-in-Motion Manual, Fourth edition.* Ljubljana: ZAG, Cestel.